12-1-1999

Polyphase tectonics and metamorphism and their relation to movement on the Monte Largo shear zone in the Manzano Mountains, central New Mexico

Douglas A. Raszewski

Polyphase Tectonics and Metamorphism and their relation to movement on the Monte Largo shear zone in the Manzano Mountains, Central New Mexico.

Douglas A. Raszewski

Senior Thesis

Department of Earth and Planetary Sciences
University of New Mexico
Albuquerque, NM

December 1999

Dr. Jane Selverstone ____________________

Dr. Karl Karlstrom ____________________

Dr. Laura Crossey ____________________

Abstract

The Proterozoic rocks of the Manzano Mountains of Central New Mexico preserve evidence of multiple deformation events. The dominant foliation is the northeast-trending S_2 that overprints the older S_1 foliation in most places. Later S_3 fabrics are present in many areas as well as S_4 crenulations in rocks from Monte de Abajo Canyon. Petrographic and field studies were performed on rocks from Monte Largo Canyon, which contains the Monte Largo shear zone, and rocks from Monte de Abajo Canyon ~3 km south of the shear zone. These studies were done to help constrain the timing of the movement on the shear zone as well as to explain the deformation and metamorphism related to movement.

From these studies it was recognized that: 1) multiple generations of top-to-the-northwest shear sense implies that there were multiple episodes of movement on the shear zone, 2) metamorphic minerals in the upper plate (south of the shear zone) indicate amphibolite facies conditions, 3) these minerals overgrew earlier S_1 and S_2 fabrics that probably developed during shearing, but were synchronous with development of S_3 fabrics that were formed during reoccurring movement on the shear zone, and 4) some deformation continued after mineral growth.

Introduction

The Monte Largo shear zone (MLSZ) is a major top-to-the-northwest thrust-sense shear zone in the Manzano Mountains of central New Mexico. The purpose of this paper is to describe fabric relations in rocks from Monte Largo Canyon, which contains the shear zone, and Monte de Abajo Canyon, south of the shear zone. These studies involved examination of rocks in the field as well as extensive examination of thin sections. My goal is to further document the shear sense and kinematic history of the MLSZ and to describe and provide explanations for deformation and mineral growth patterns in and adjacent to the MLSZ.

Geologic Setting

The Manzano Mountains of Central New Mexico are an east-tilted Tertiary fault block that forms the east flank of the Rio Grande Rift. They have spectacular exposures of Proterozoic metasedimentary, metavolcanic, and plutonic rocks uncomfortably overlain by Paleozoic sedimentary rocks. The mountain range is ~70 km long and ~15 km wide. The Precambrian rocks are made up of multiply deformed metarhyolites, pelitic schists, quartzites and amphibolites, some of which yield U-Pb zircon dates of ~1.65 Ga (Bauer et al., 1983). The area discussed in this study (fig. 1) is bounded by Sapo Canyon in the north and Monte de Abajo Canyon in the south. However most work was done just south of Sapo Canyon in Monte Largo Canyon where the the Monte Largo shear zone is exposed.

The Monte Largo shear zone (MLSZ), first named by Thompson et al. (1991), is a northeast-striking (010--050) and southeast-dipping ($50-80^{\circ}$) zone of mylonitic rocks. The shear zone separates greenschist grade to the north from amphibolite grade to the south. Metamorphic rocks on both sides of the shear zone include quartzites, meta-pelitic rocks (Blue Springs Schist), mafic schist, amphibolites and metarhyolites (Sevilleta Metarhyolite).

Previous Work

The Monte Largo shear zone was first recognized in Monte Largo Canyon by Bauer (1988) as a 2-m-wide ductile fault. Thompson et al. (1996) recognized a wider zone of ductile deformation and mapped the MLSZ on the basis of contrasts in metamorphic facies and deformation style. They noticed that the MLSZ separates the southern, lower amphibolite facies rocks (~530°C) from the northern, greenschist facies rocks (~485°C). Kyanite was recognized as the only Al_2SiO_5 polymorph in aluminous quartzite near the boundary and is suggestive of pressures above 2.5 kbar and temperatures above 400°C. Even though the shear zone is mapped as the boundary between the two different metamorphic facies, deformation associated with its movement has affected an area at least 2 km wide. Thompson et al. (1991) recognized kinematic indicators that indicate top-to-the-northwest thrust sense with higher grade amphibolite facies rocks (hanging wall) to the south thrust over the lower grade greenschist facies rocks (footwall) to the north.

Northrup (1991) studied the geochemical fluid-rock interactions within the Monte Largo shear zone and noticed hydrothermal veining had occurred at several stages in the deformational history. His studies showed that early quartz veining was pervasively distributed and produced large numbers of small veins, whereas later veining was more continuous and had fewer, larger veins. The early veins show little wallrock alteration, with fluids low in salinity and CO_2. In contrast, later veins had higher salinity and CO_2 content and show increased amounts of wallrock alteration. He concluded that vein formation occurred at progressively lower P-T conditions and therefore tracked the unroofing of the shear zone from a ductile to a brittle regime.

In their studies of the Manzano Mountains, Bauer et al. (1993) concluded that major D_2 deformation occurred sometime between the emplacement of the ~1.65 Ga Monte Largo pluton and the ~1.4 Ga Priest pluton. This interpretation was based on fabric relations and U-Pb zircon geochronology. They showed that the Monte Largo pluton is foliated and contains three distinct fabrics that also exist outside of the pluton margin. The dominant structures in the range are tight to isoclinal, gently to moderately plunging second-generation F_2 folds that fold layer-parallel S_1 schistosity (Bauer et al., 1993). They noted that an S_1-parallel foliation is especially intense in mylonitic granite along the margin of the pluton and that it shows top-to-the-northwest shearing. It is believed that the pluton and country rock were deformed together during north-directed D_1 deformation. S_2 crenulations that are axial planar to the F_2 antiforms are representative of the second phase of deformation. Also they noticed late, low-angle, top-to-the-northwest S_3 shear bands. Bauer et al. (1993) state that D_2 and D_3 structures indicate that thrusting and shortening post-dated crystallization of the Monte Largo pluton. The evidence for deformation prior to emplacement of the Priest pluton is similar to that presented by Thompson et al. (1996) that will be outlined below. Bauer et al. (1993) therefore believe that top-to-the-northwest thrusting and shearing occurred in several phases and that it is unclear if these deformations are related or not. They could be evidence of multiple movement episodes, or only one progressive event. If the later is the case then deformation must have waned during Priest pluton emplacement (Bauer et al., 1993).

Based on the consistency of the mineralogy of the greenschist facies rocks north of the MLSZ as well as consistency in the mineralogy of the amphibolite facies rocks south of the shear zone, Thompson et al. (1996) suggested that the metamorphic conditions were regional in extent. They argued that regional greenschist-facies metamorphism of the lower plate was synchronous with, and also post-dated shear zone deformation. This is evidenced by kyanite and chloritoid crystals in alignment with the mylonitic S-C texture, meaning that they were stable during shear zone activity. Some porphyroblasts of chloritoid and garnet overgrew the mylonitic foliation, indicating that mineral growth also post-dated shearing. Thompson et al. (1996) argued that the thrusting and regional amphibolite-facies metamorphism may have occurred prior to emplacement of the 1.43 Ga Priest pluton, possibly during a period of deformation around 1.65 Ga. This interpretation is based on the occurrence of lower amphibolite facies minerals, such as kyanite, staurolite and garnet, as inclusions in somewhat higher temperature, lower pressure contact metamorphic mineral assemblages (andalusite and sillimanite) of the Priest pluton. Also present in some rocks are garnet porphyroblasts with cloudy cores and euhedral rims that overgrow S_2 foliation. This garnet texture was thought to suggest two generations of garnet growth, with the euhedral rims representing contact metamorphism by the Priest pluton. If this recrystallization was due to heating from the pluton, then thrusting, which is thought to be synchronous with amphibolite growth of the cloudy cores of the garnets, would have to be older than 1.43 Ga (Thompson et al., 1996).

Marcoline (1996) and Marcoline et al. (1999) looked at microstructures and $^{40}Ar/^{39}Ar$ thermochronology of the MLSZ. They concluded that the MLSZ, as observed in Monte Largo Canyon, is not a discrete shear zone, but just one localized high-strain zone within a larger deformation zone. They mapped other high-strain zones north of Monte Largo Canyon in Trigo Canyon and believed that these discontinuous zones of high-strain are lithologically controlled. High-strain zones trend parallel to and are adjacent to the contact between the Blue Springs schist and the Sevilleta metarhyolite. Marcoline et al. (1999) argued that greenschist facies metamorphism and deformation occurred during the ~1.6 Ga event and that greenschist-amphibolite transition zone and amphibolite facies metamorphism and deformation occurred during a ~1.4 Ga event (Marcoline et al., 1998). They proposed that there were two distinct deformational events as opposed to one progressive deformational event.

This interpretation is based on their petrographic and chemical studies of schists, quartzites and amphibolites along with $^{40}Ar/^{39}Ar$ geochronology of amphiboles. In the Blue Springs Schist they found microscopic folds and S-C fabrics with asymmetries consistent with southeast-side-up movement; these fabrics are microstructurally distinct from earlier deformational fabrics. They find consistent grain-shape preferred orientations of top-to-the-northwest in quartz mylonites from near the shear zone. In amphiboles they see a relict actinolite foliation cross-cut by a foliation defined by aligned hornblende, as well as hornblende rimming actinolite porphyroclasts and fragments. $^{40}Ar/^{39}Ar$ age spectra on syn-kinematic hornblende grains show closure to argon loss by ~1.4 Ga (Marcoline et al., 1999). They note that actinolite also gave similar ages, but this is expected because they were degassed of ^{40}Ar during hornblende growth as well. These age data, combined with microstructural information, such as S_2 mylonites and kinematic indicators, led Marcoline to argue that top-to-the-northwest movement on the MLSZ must have been during the ~1.4 Ga deformational event.

Shear Sense

The number of fabrics present in any particular rock can vary between 1 and 4. The earliest tectonic fabric, S_1, is a bedding-parallel foliation in the supracrustal rocks. This supracrustal package is thought to have been folded into large-scale, upright, F_2 folds, which resulted in the northeast-trending composite S_1/S_2 fabric that dominates the supracrustal rocks in the area (Thompson et al., 1996). The third and fourth fabrics are northeast-striking fabrics and are represented by crenulations and shear bands that kink and crosscut the earlier S_1/S_2 fabric. The shear sense indicators present in some of these fabrics suggest that deformation is related to movement on the MLSZ.

Numerous rocks from in and around the shear zone contain excellent shear sense indicators. Even locations as far south as Monte de Abajo Canyon contain kinematic indicators. All of these kinematic indicators give overwhelming evidence for top-to-the-northwest movement on the MLSZ. This section further documents this shear sense and shows that this movement took place on S_2, on S_3 and as reactivation's of the earlier S_1/S_0 fabric.

The best evidence of shear sense comes from asymmetric grains and S-C fabrics and, to a lesser extent, shear bands and crosscutting fabric relations. In schistose quartzites from just south of the MLSZ, large quartz porphyroclasts as well as small quartz and opaque grains aligned in the S_2 matrix are elongate and sigmoidal. In samples K99-ML-4 and K99-ML-7 all asymmetry gives top-to-the-northwest sense of movement (figs. 2-4). In K99-ML-4, later S_2 or S_3 shear bands are present that further confirm southeast-side-up movement (fig. 5).

Other schistose quartzite samples from near the MLSZ (J-11 and J-16) show evidence of shear sense within the S_2 mica bands that overprint the S_1 fabric. J-11 contains numerous small chloritoid grains that are sigmoidal as well as S_3 shear bands (fig. 6). In the mica band of J-16, shear sense is seen in small sigmoidal quartz grains as well as in the way that the S_1 fabric is bent into the crosscutting S_2 fabric (fig. 7). All evidence is consistent with southeast-side-up movement.

Evidence for top-to-the-northwest sense of shear exists north of the MLSZ as well. Sample J-10, a mylonitic metarhyolite located about 100 meters north of the shear zone contains some asymmetric quartz grains, but the best evidence comes from a sigmoidal carbonate grain with tails giving top-to-the-northwest shear sense (fig. 8). Sample YA-92-4 is a pelitic schist from ~.5 km north of the shear zone that has asymmetric quartz grains as well as S-C fabrics that both give northwestward vergance (fig. 9). The fabrics in both of these samples are believed have been formed during S_2 deformation.

Rocks further from the MLSZ also show evidence for southeast-side-up shearing. Sample J-18, a garnet schist located about 1 km south of the shear zone, contains well-developed shear sense where S_1 bends into S_2 shear zones and S_3 shear bands crosscut S_2 foliation giving southeast-side-up movement on this fabric as well (fig. 10). Even rocks from Monte de Abajo Canyon, which is located about 3 km south of the MLSZ, contain evidence for top-to-the-northwest sense of shear. Quartzite sample JA-28 contains only one foliation that has many dextral quartz porphyroclasts and small quartz grains that are consistent with this movement (fig. 11). Another quartzite from the same area showing only one foliation contains an oxide band with grains that have a preferred orientation indicating top-to-the-northwest shear (fig. 12). An amphibolite from Monte de Abajo Canyon also shows evidence of southeast-side-up movement: Figure 13 shows a hornblende porphyroblast, which grew during amphibolite facies metamorphism, with a biotite tail on its upper right corner and a hornblende tail being dragged out on its lower left corner. No other amphibolites give any such evidence of shearing.

In conclusion, all of the above mentioned evidence shows southeast-side-up sense of shear on the MLSZ. The majority of these kinematic indictors are located in the S_2 foliation indicating that movement happened during D_2 deformation. However, S_3 shear bands also were noted to have top-to-the-northwest movement, meaning that there were multiple movements on the MLSZ at different times. This theory is further supported by the fabric relations that are present in rocks from Monte Largo and Monte de Abajo canyons.

Fabric Development

Multiple fabrics such as foliations, crenulations and shear bands are present in the Proterozoic rocks of the Manzano Mountains. The foliations occur ubiquitously, whereas the crenulations are best represented in the pelitic rocks of Monte de Abajo Canyon. Shear bands are present in many locations throughout the study area. These fabrics, combined with porphyroblast-matrix relations, allow us to reconstruct the polyphase tectonism history of these rocks.

Samples were studied in thin section to evaluate the microscale relationships between these fabrics and growth of metamorphic minerals. Of the thin sections made, 9 samples were picked out that expressed multiple fabrics. Four samples [1 garnet schist (J-18) and 3 schistose quartzites (J-11, J16 & K99-ML-6)] were from Monte Largo Canyon within and just south of the MLSZ. These rocks were studied to understand the deformation fabrics that are present near the shear zone. Five samples, all garnet-chloritoid schists (JA-33, JA-34, JA-35, JA-36 & JA-37), were from Monte de Abajo Canyon in the upper plate of the shear zone ~3 km south of the MLSZ. These rocks were studied to understand the character of deformation and metamorphism in areas away from the shear zone.

Fabric relations from rocks in Monte Largo Canyon.

The earliest fabric seen in all samples from Monte Largo Canyon is believed to be the S_1. In samples J-11, J-16 and J-18 (fig. 14c, 214b & 14d respectively) it is represented by aligned elongate quartz grains and mica grains and strikes northeast with a nearly vertical northwesterly dip. In all of these samples the S_1 is truncated and bent into the dominant S_2 fabric. In sample K99-ML-6, S_1 is a bit different. S_1 is represented by aligned mica layers oriented along what is thought to be the original bedding, S_0. These layers are perpendicular to and crenulated by the S_2 foliation (fig. 14a). This gives S_0/S_1 a shallow northwesterly dip, as opposed to the other samples.

In the thin section of sample J-18 two garnets are present. Although both garnets have the S_2 foliation wrapping around them, one is almost euhedral whereas the other is subhedral with an elongation and chlorite pressure shadows in the S_1 direction (fig. 15). Quartz and mica inclusions in these garnets trend north-south and are oriented perpendicular to S_1 and about 45^0 to S_2 (fig. 15). These inclusions in the garnets are very peculiar since they are pre-garnet growth but are perpendicular to S_1. They are believed to be remnants of some earlier pre-S_1 fabric that is not expressed anywhere else, and they are therefore labeled $S_{1(a)}$. These earlier inclusions, along with the elongation of the garnet in the S_1 foliation direction, gives evidence that the garnet growth in J-18 was syn-$S_{1(b)}$.

Although S_1 and S_2 are recognized to be a composite fabric in most of the study area, they are not parallel in and around F_2 fold hinges. The offsetting S_1 and S_2 fabrics in these samples are assumed to be representative of such areas. In all four of the samples from Monte Largo Canyon the dominant fabric is the northeast-trending, southeast-dipping S_2 foliation. In three of the samples (J-11, J-16, & J-18), this fabric is evidenced as bands of aligned mica that clearly crosscut and deflect, with top-to-the-northwest shear sense, the earlier S_1 fabric (fig. 14c, 214b & 14d respectively). In sample K99-ML-6, the dominant S_2 fabric is represented by quartz and mica layers that are perpendicular to and crenulate the earlier S_0/S_1 mica fabric (fig. 14a). Because this sample is from a hinge region of a major F_2 fold south of the shear zone, it implies that S_2 shearing was accompanied by northwest-southeast contraction.

The S_3 fabric is also present in all four of these samples, although it is not expressed the same in all samples, all suggest continued northwest directed thrusting. In J-11, S_3 is represented by crenulations with northeast-striking southeast-dipping axial planes (fig. 14c), and in J-18 by northwest-verging, shallowly dipping shear bands (fig. 14d). These are similar to those reported by Bauer et al. (1993) and indicate continued top-to-the-northwest shear sense during S_3. In J-16, S_3 is represented by folds in the S_1 and S_2 fabrics (Fig 16). The axial plane of these folds is almost vertical and approximately parallel to S_1, with the asymmetry indicating continued northwest vergance. Although all three of these S_3 fabrics do show top-to-the-northwest thrust sense, the difference in orientation of S_3 in J-16 as opposed to J-11 and J-18 indicates that S_3 is either expressed differently in different areas depending on preexisting anisotropy, or that different deformation events affected these areas.

In K99-ML-6, S_3 is represented by reactivation along S_1 where the S_2 quartz and mica fabric are bent into the S_0/S_1 mica layers giving southeast-side-up movement sense (fig. 14a). Because the layers are crenulated by S_2, they must be younger, which means that since S_2 bends into these layers in some places, that is is most likely due to reactivation along S_1 during S_3 deformation.

Garnet is also present in samples J-16 and K99-ML-6 (fig. 14b & 14a). The garnets in these samples are elongate and anhedral and only overgrow S_1 and S_2, as evidenced by their shape (fig. 14 a & b). However, in K99-ML-6, the S_2 fabric of the mica is external to the garnets and wraps around them. This is most likely due to reactivation during S_3. The quartz grains inside the garnets are only mildly elliptical whereas quartz grains outside are stretched out in the S_3 direction. It is believed from these relations that the garnets grew post-S_2, which initiated annealing of the quartz inside and nearby the garnet. The grains outside the garnets were continually elongated, probably during the S_3 deformation period.

The euhedral and subhedral garnets in J-18 and the anhedral garnets in J-16 and K99-ML-6 give somewhat conflicting timing information and it is unclear if their growth is related to one another. However, the difference in garnet shape and timing of growth could be because of the difference in the original composition of the rocks. J-16 and K99-ML-6 are schistose quartzites, whereas J-18 is a pelitic schist.

Fabric relations in rocks from Monte de Abajo Canyon.

The S_1, S_2 and S_3 fabrics in the rocks from Monte de Abajo Canyon are believed to be the same as the fabrics expressed in Monte Largo Canyon with the addition of an S_4 crenulation. The relative timing of mineral growth and development of fabrics, however, is different than in Monte Largo Canyon.

In all five samples from Monte de Abajo Canyon the dominant fabric is the northeast-striking, southeast-dipping S_2 fabric. This S_2 fabric is represented by aligned mica and quartz grains that crenulate, bend and truncate the older S_1 fabric. In microlithons containing S_1, mica grains are oriented at a high angle or perpendicular to the S_2 fabric and are crenulated with S_2 as the axial plane in samples JA-33, JA-34 and JA-35 (figs. 14e, 14f & 14g respectively). The S_3 fabric is represented by northeast-to east-striking crenulations of the S_2 fabric and is present in all five samples (figs. 14e-i). The S_4 fabric is expressed as tight kink bands that are predominantly present only around porphyroblasts. The orientations of these kink bands vary from sample to sample.

Garnet and chloritoid occur in all five rocks, along with staurolite in JA-36 and JA-37. In cross-sectional views of JA-33, JA-34 and JA-35 (figs. 14e-g) the garnets have inclusions of quartz, mica and opaques that are aligned with the dominant S_2 foliation, indicating that they overgrew S_2. However in plan-view sections of JA-36 and JA-37 (figs. 14h-i) the inclusion trails of the garnets and staurolites are oriented ~35° from the main foliation and these porphyroblasts thus either overprint an older fabric or have been rotated, meaning that some deformation outlasted mineral growth. Chloritoid contains inclusions of quartz, mica, opaques, garnet and staurolite. The quartz, mica and opaque inclusions in the porphyroblasts show the same S_3 crenulation as outside of the minerals, but the bends seem to be broader in some places, suggesting that mineral growth was syn-S_3. This is best expressed by the opaque inclusions in chloritoid (fig. 17). Nowhere do the inclusions seem to be as tightly crenulated as the S_4 crenulations.

The growth of garnet and staurolite most likely occurred during formation of the S_3 crenulations. This is evidenced by the fact that the inclusion trails in the porphyroblasts are bent just the same as the broad crenulations outside the porphyroblasts (fig. 17). Since all of the bends of the inclusions are generally broad with no evidence of tight kinks (fig 14g), S_4 fabric development is most likely later than all mineral growth. It should also be noted that since garnet and staurolite are present as inclusions in the chloritoid, the chloritoid growth is believed to be slightly later, but could also be from a much younger event.

The key to the deformation history in this area is the rotated inclusion fabrics in the garnets of JA-36 and JA-37. Because these inclusions are in this pattern only within the garnets, it is suggested here that the garnets rotated during or after their growth, implying that there was continued deformation, probably related to movement on the MLSZ, during S_3 development. The S_4 kinking appears to be due to this same movement. In fact, it is quite possible that S_3 development, mineral growth, mineral rotation and S_4 development are one related progressive deformation event.

The evidence for this is that the tight S_4 crenulations are present only around the margins of the porphyroblasts and on top of the broad S_3 crenulations, as well as the fact that the crenulations are much broader inside the porphyroblasts than outside (fig. 17). It is proposed here that S_3 crenulations were developed first, then porphyroblast growth, followed by rotation of garnet and staurolite. The rotation coupled with the strengths of garnet, staurolite and chloritoid in relation to mica was responsible for the tightening of the S_3 crenulation, as well as formation of new, tight S_4 crenulations. The randomness of the S_4 crenulation orientations can also be explained if their development was not completely controlled by the regional stress field, but also by their relation to nearby stronger garnet and staurolite grains.

Metamorphic Facies

The Monte Largo shear zone separates two distinct metamorphic facies: The upper plate to the south contains rocks of amphibolite grade metamorphism whereas the lower plate to the north contains rocks of greenschist grade metamorphism. These differences are noticeable in mafic as well as in pelitic rocks throughout the area. Thompson et al., (1996) noted that these metamorphic facies were regional in extent, separated only by the MLSZ.

The main difference in the mafic rocks in the area is the existence of actinolite north of the shear zone and hornblende south of it. Mafic metavolcanics in the lower plate contain the assemblage actinolite, epidote, albite, chlorite and rare biotite (Thompson et al., 1996). Along with quartz, this assemblage has been recognized to be representative of the greenschist facies (Bucher and Frey, 1994; Apted and Liou, 1983). On an ACF diagram this assemblage would plot inside the triangle with epidote, chlorite and actinolite at the corners (fig 18a). This assemblage is is consistent with temperatures below about 500°C (Bucher and Frey, 1994).

Mafic metavolcanic rocks in the upper plate contain the assemblage hornblende, plagioclase, $\pm$ chlorite, $\pm$ epidote, $\pm$ biotite and $\pm$ actinolite. This assemblage represents the epidote amphibolite to amphibolite facies (Bucher and Frey, 1994; Apted and Liou, 1983). On an ACF diagram these assemblages plot inside the hornblende-epidote-chlorite and hornblende-chlorite-actinolite triangles (Fig. 18b). Temperatures at which these assemblages are stable are in the 500-550°C range (Bucher and Frey, 1994; Spear, 1993).

Pelitic schists from Monte de Abajo Canyon in the upper plate are also representative of amphibolite facies. These rocks have the assemblage white mica, quartz, chlorite, feldspar, garnet, ± staurolite, ± biotite and ± chloritoid. This assemblage, especially the rocks that contain both garnet and staurolite, plot on AFM diagrams M-k through M-o of Spear (1993) (fig. 19). The reason for this kind of diagram is to show the types of mineral assemblages that may be encountered at different P-T conditions. Reaction (10-15) marks the first appearance of staurolite in low-Al pelites introducing diagram M-k, while reaction (10-16) marks the first appearance of kyanite in low-Al pelites and plots in diagram M-l (Spear, 1993). Reaction (10-17) introduces diagram M-m and brings about the disappearance of chlorite in pelitic rocks. Reaction (10-18) is the phase transition of the aluminosilicates where sillimanite replaces kyanite in diagram M-n (Spear, 1993). The next two reactions (10-19 & 10-20) bring about the demise of staurolite. Reaction 10-19 leaves staurolite as an interior phase (diagram M-o) and reaction 10-20 is the complete removal of staurolite from the assemblage (Spear, 1993). These diagrams correspond to temperatures of ~550-700°C and pressures between ~3 and 14 kbar (fig. 20). The reason the pressure range is so large is that all three aluminosilicate polymorphs are present near the Priest pluton (Thompson et al., 1996) and sillimanite and andalusite found in rocks throughout the region (Karlstrom, personal comm.). However no aluminosilicates were found in the rocks in this study. Based on mineral assemblages of other rocks the pressures are most likely below 6 kbar, and probably exist near the aluminosilicate triple point (fig. 20).

Discussion

Neither deformational fabrics nor metamorphic mineral assemblages can safely be used as "time lines" to reconstruct tectonic events. For example, the dominant fabric in one area may not have formed at the same time as a dominant fabric in another area even if they represent the same "generation", and particularly if the different areas could have undergone different numbers and intensities of deformations. Similarly, metamorphic minerals that exist in different regions can grow at different times depending on bulk composition, fluids and P-T path. For example, garnet-bearing rocks from different areas can capture different times and P-T conditions of metamorphism.There is also the possibility that two grains of the same minerals in a rock can exhibit different shapes. The garnets in sample J-18 are evidence of this. Even though they are probably from the same period of growth, they have different shapes. Likewise, cores and rims of the same mineral may record events separated by 200 Ma (Thompson et al., 1996). When trying to unravel such complicated histories in areas with multiple deformation fabrics, all of these possibilities must be kept in mind.

In the rocks of Monte Largo Canyon we have three generations of fabrics, with garnet growth placed at post-S_2 in a few samples, and syn-S_1 in another sample. This problem can be explained by the fact that the rocks with different garnet growth have different bulk compositions and the garnets may thus have grown at different P-T and time conditions. In the rocks from Monte de Abajo Canyon we have four generations of fabrics (with S_3 and S_4 interpreted to be part of one progressive deformation), with mineral growth placed at syn-S_3. Because growth of garnet and staurolite is representative of amphibolite facies conditions, this puts at least some of the amphibolite metamorphism of the upper plate as post-S_2 and syn-S_3, possibly in agreement with Thompson et al. (1996) who noted that amphibolite grade metamorphism around the Priest pluton was superimposed on earlier pre-pluton penetrative features.

A possible explanation for this is that the growth of amphibolite grade minerals was related to emplacement of the Priest pluton, which was synchronous with renewed S_3 movement on the shear zone. Thompson et al. (1996) noted that there is not a sharp boundary between the regional amphibolite grade metamorphism and the contact metamorphism, and hence, that all amphibolite grade metamorphism could be related to pluton emplacement. It has also been noted that regional 1.4 Ga metamorphism is amphibolite grade in many areas throughout the southwest (Karlstrom et al., 1997). The subsurface geometry to the Priest pluton is unknown and it is possible that it exists not

Qpa **Piedmont deposits, undivided (Pleistocene-Holocene)** – Undivided deposits of units **Qa**, **Qpm**, and **Qpo**. Mostly clast-supported gravel and dominated by granite and metamorphic rocks exposed east of the Manzano Mountains drainage divide. Deposits are locally matrix-supported near mountain front. Locally entrenched near mouths of mountain-front drainages. Base not observed west of the mountain front. Estimated thickness ranges from 1 m to more than 10 m.

Qpm **Middle piedmont deposits (middle Pleistocene)** – Brown to dark yellowish-brown, poorly consolidated, poorly sorted, cobble to boulder gravel and sand. Forms broad, slightly dissected constructional surfaces that are inset against unit **Qpo**. Deposits contain clast- and matrix-supported gravels. Soils are moderately to strongly developed. Base not exposed, but is at least 3 m in thickness.

Qpo **Older Piedmont deposits (lower to middle Pleistocene)** – Poorly consolidated, clast- and matrix-supported gravel and sand with sparse silt and clay. Deposits are dominated by pebbly to locally bouldery gravel containing abundant granite and metamorphic rocks. Forms deeply dissected hills near western front of Manzano Mountains where unit may represent younger aggradational units of the Santa Fe Group. Base not observed west of the Manzano Mountains, but is at least 6 m thick.

Qp2 **Eastern-slope deposits (middle Pleistocene)** – Poorly consolidated, cobble to boulder gravel and sand. Forms moderately dissected, upper plate, as evidenced by mineral assemblages in amphibolites and schists. This movement was possibly related to emplacement of the Priest pluton, and included growth of garnet and staurolite with chloritoid growth sometime after. Following this was continued tightening of S_3 crenulations and rotation of garnet porphyroblasts that were either part of the same progressive event or a later period of deformation (S_4). Top-to-the-northwest shear sense is present in both the S_2 and S_3 deformation fabrics, which is evidence of movement on the MLSZ and is consistent with earlier studies.

Acknowledgments-- I would like to thank Jane Selverstone and Karl Karlstrom for all of their help and support and for their helpful review of this paper. I would also like to thank Sara Dieffenbach for all of her wonderful love and support. This research was partly funded by NASA PURSUE grant #64.

References

Apted, M. J. and Liou, J. G., 1983. Phase relations among greenschist, epidote-amphibolite, and amphibolite in a basaltic system: American Journal of Science, v. 283-A, p. 328-354.

Bauer, P. W., 1982. Precambrian geology and tectonics of the southern Manzano Mountains, Central New Mexico: New Mexico Geological Society, Guidebook to the 33rd Field Conference, p. 211-216.

Bauer, P. W., Karlstrom, K. E., Bowring, S. A., Smith, A. G., Goodwin, L. B., 1993. Proterozoic plutonism and regional deformation - new constraints from the southern Manzano Mountains, Central New Mexico: New Mexico Geology, v. 15, no. 3, p 49-56.

Bucher, K., and Frey, M., 1994. Petrogenesis of metamorphic rocks: Springer Verlag, Berlin. 6th edition. 318 p.

Karlstrom, K. E., Dallmeyer, R. D., Grambling, J. A., 1997. $^{40}Ar/^{39}Ar$ evidence for 1.4 Ga. regional metamorphism in New Mexico: Implications for thermal evolution of the lithosphere in the Southwestern USA: Journal of Geology, v. 105, p. 205-223.

Marcoline, J. R., 1996. Field, petrographic, and $^{40}Ar/^{39}Ar$ constraints on the tectonic history of the Central Manzano Mountains, Central New Mexico [MS Thesis]: Socorro, New Mexico Institute of Mining and Technology, 124 p.

Marcoline, J. R., Heizler, M., Goodwin, L. B., Ralser, S., Clark, J., 1999. Thermal, structural and petrological evidence for 1400 Ma metamorphism and deformation in Central Mew Mexico: Rocky Mountain Geology, v.34, p. 93-119.

Northrop, C. J., 1991. Thermal, chemical, and structural characteristics of fluid migration and fluid-rock interactions in a Mid-Proterozoic shear zone, Manzano Mountains, New Mexico [MS Thesis]: Tucson, University of Arizona, 126 p.

Spear, F. S., 1993. Metamorphic phase equilibria and pressure-temperature-time paths: Mineralogical Society of America. Washington D. C. 779 p.

Thompson, A. G., Grambling, J. A., Dallmeyer, R. D., 1991. Proterozoic tectonic history of the Manzano Mountains, Central New Mexico: New Mexico Bureau of Mines and Mineral Resources Bulletin, v. 137, p. 71-77.

Thompson, A. G., Grambling, J. A., Karlstrom, K. E., Dallmeyer, R. D., 1996. Mesoproterozoic metamorphism and $^{40}Ar/^{39}Ar$ thermal history of the 1.4 Ga Priest pluton, Manzano Mountains, New Mexico: The Journal of Geology, v. 104, p. 583-598.

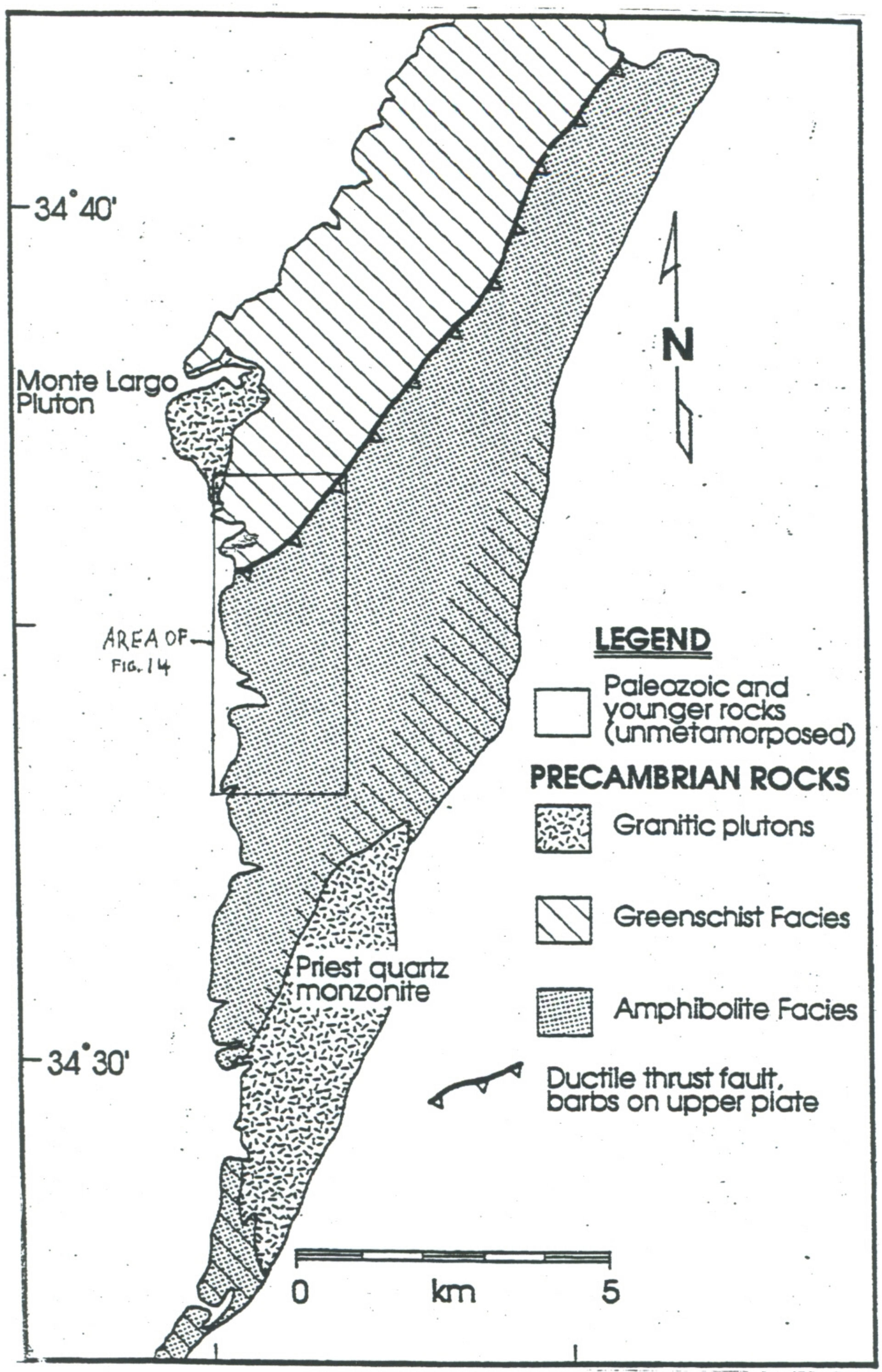

Figure 1. - Geologic map of Proterozoic rocks in Manzano Mountains showing location of study area.

Figure 2. - Sample K99-ML-4: Cross-sectional view, looking NE showing S, C and C' in schistose quartzite of MLSZ. Gives top-to-NW shear sense. (2.5X; cross polars)

Figure 3. - Sample K99-ML-4: Cross-sectional view, looking NE showing S and C in schistose quartzite of MLSZ and displaced quartz grain. Gives top-to-NW shear sense. (2.5X; cross polars)

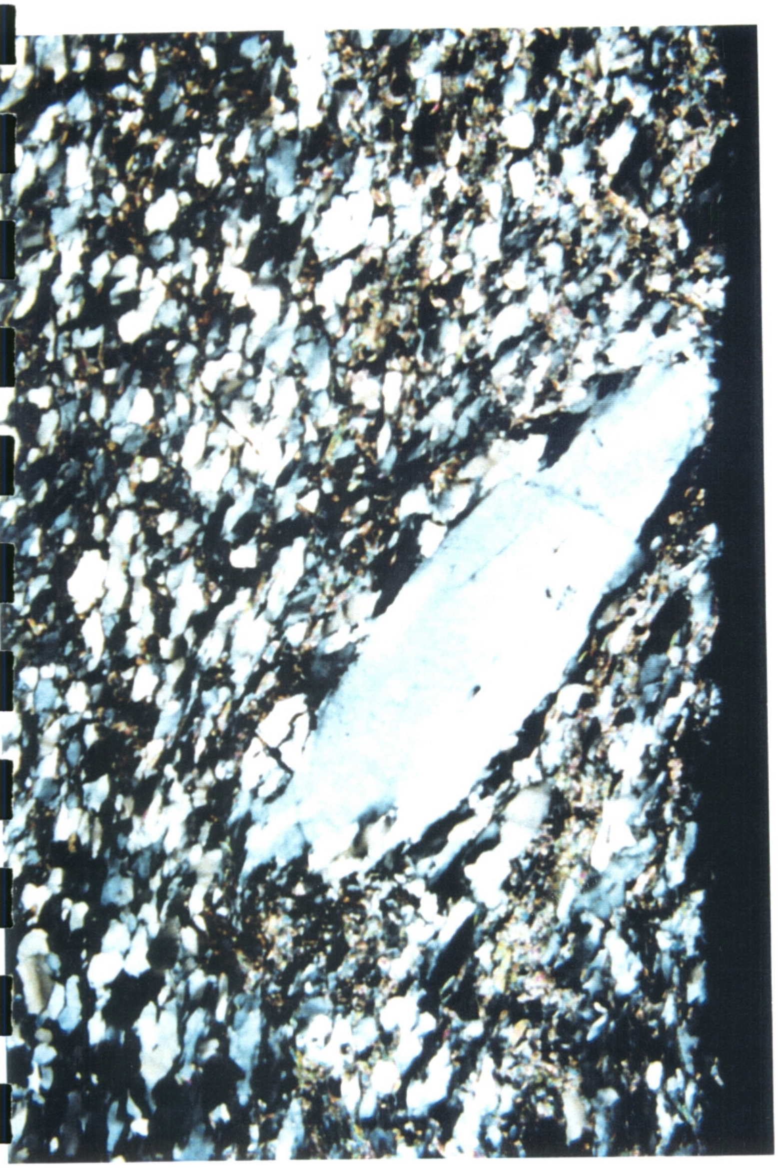

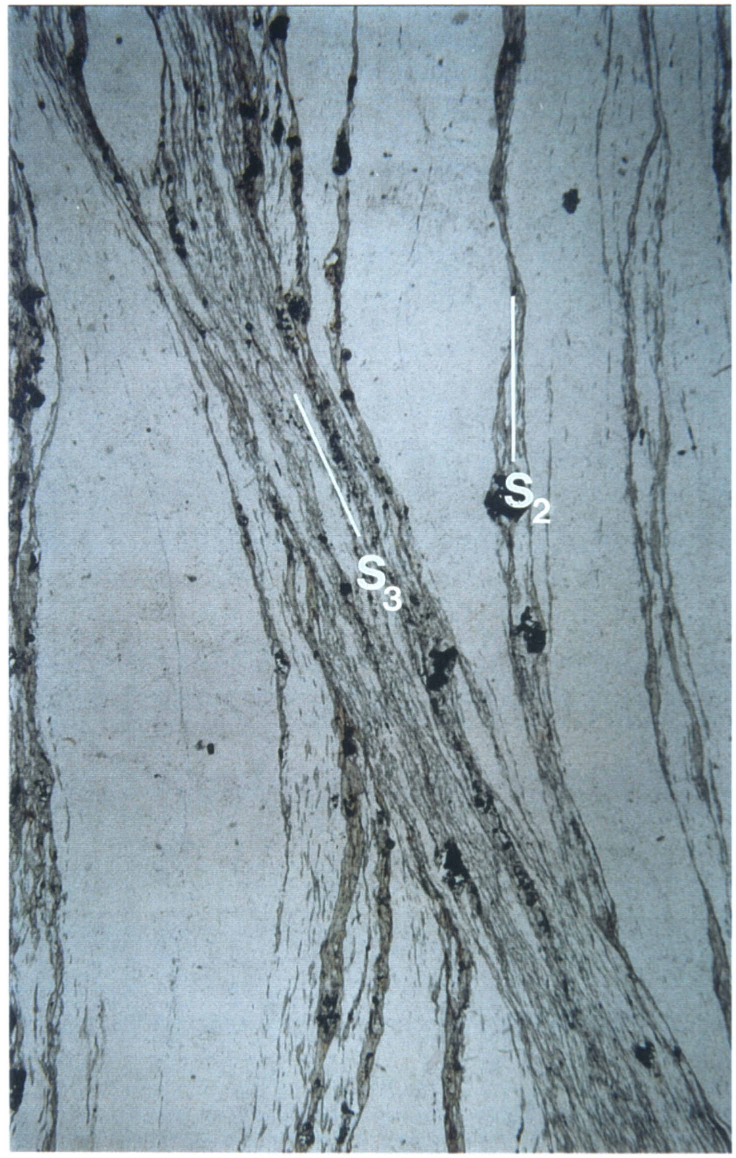

Figure 4. - Sample K99-ML-7: Cross-sectional view, looking NE showing asymmetric quartz porphyroclast and matrix grains in schistose quartzite S of MLSZ. Gives top-to-NW shear sense. (2.5X; cross polars)

Figure 5. - Sample K99-ML-4: Cross-sectional view, looking NE showing S_3 shear band in schistose quartzite of MLSZ. Gives-top-to-NW shear sense. (2.5X; plain light)

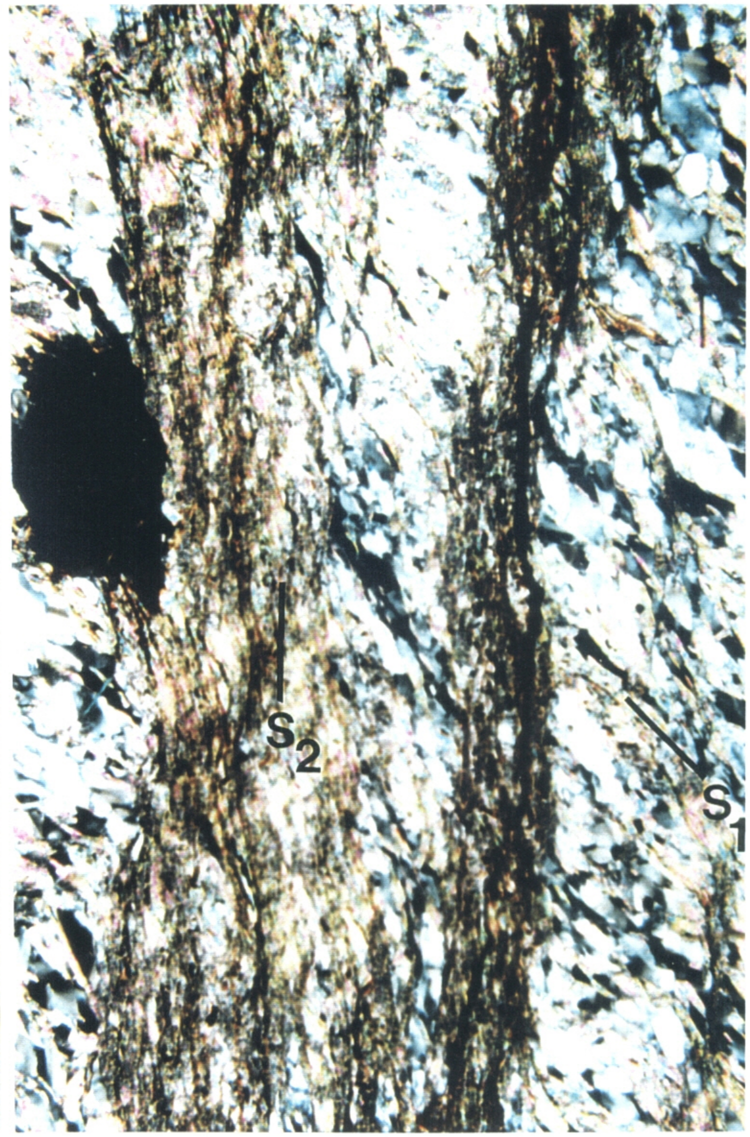

Figure 6. - Sample J-11: Cross-sectional view, looking NE showing sigmoidal chloritoid grains and C' planes in S_2 foliation in schistose quartzite S of MLSZ. Gives top-to-NW shear sense. (10X; plain light)

Figure 7. - Sample J-16: Cross-sectional view looking SW showing S_1 foliation being offset and bent into the S_2 foliation in schistose quartzite S of MLSZ. Gives top-to-NW shear sense. (2.5X; cross polars)

Figure 8. - Sample J-10: Cross-sectional view looking SSW showing a sigmoidal carbonate grain in quartzite N of MLSZ. Gives top-to-NW shear sense. (5X; cross polars)

Figure 9. - Sample YA-92-4: Cross-sectional view looking NE showing a sigmoidal chlorite grain and S-C fabric in mica schist N of MLSZ. Gives top-to-NW shear sense. (2.5X; plain light)

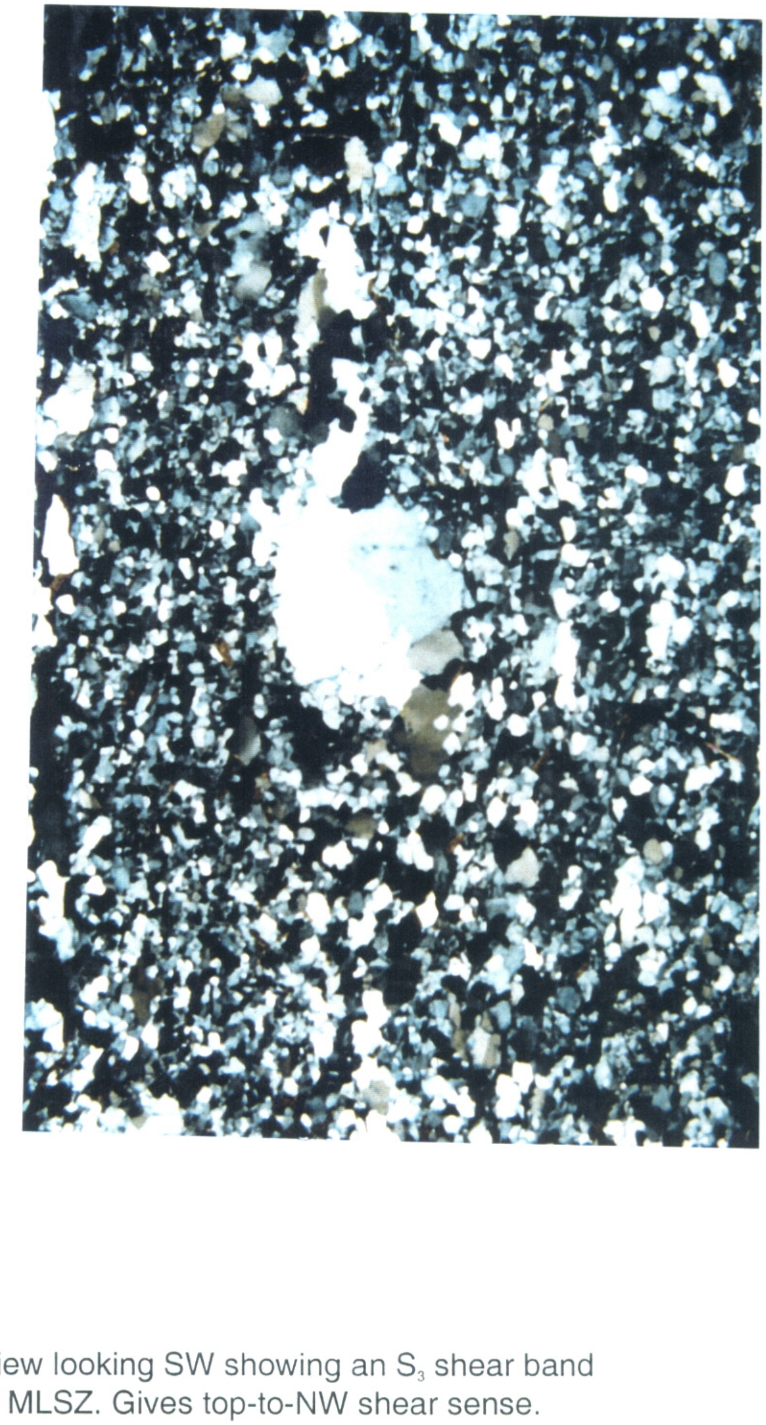

Figure 10. - Sample J-18: Cross-sectional view looking SW showing an S_3 shear band crosscutting S_1 and S_2 foliation in schist S of MLSZ. Gives top-to-NW shear sense. (2.5X; Plain light)

Figure 11. - Sample JA-28: Cross-sectional view looking SW showing a sigmoidal quartz porphyroblast in a quartzite from Monte de Abajo Canyon. Gives top-to-NW shear sense. (2.5X; cross polars)

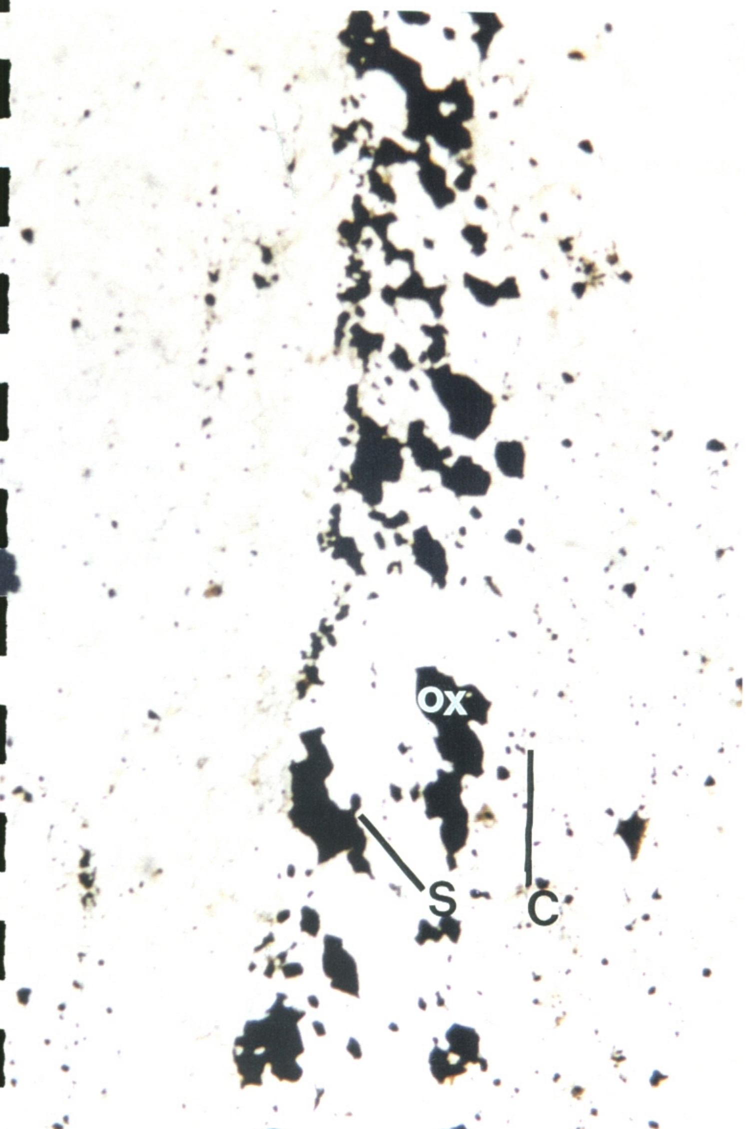

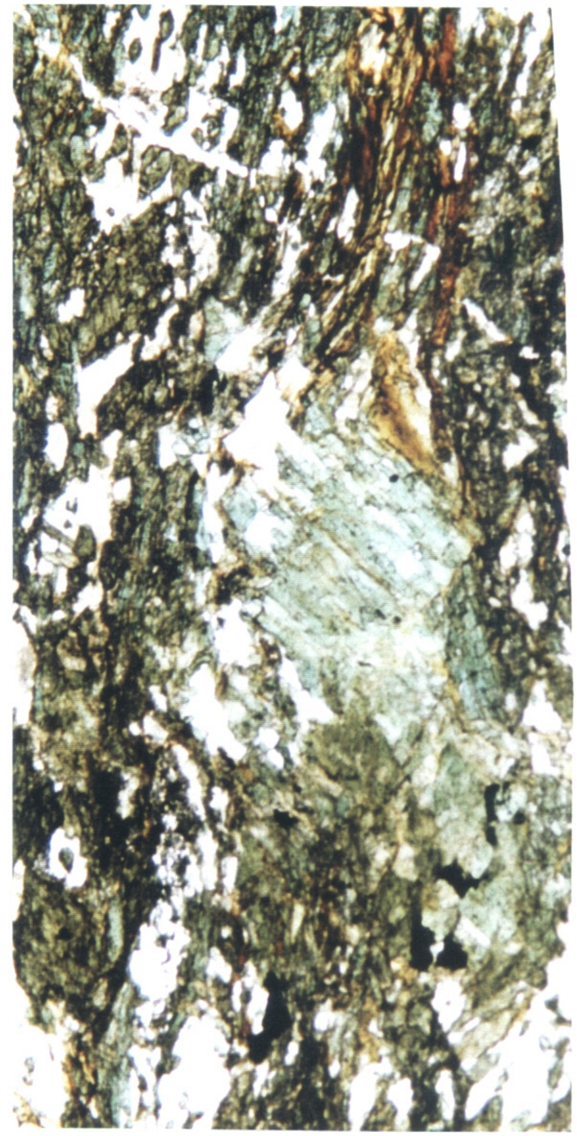

Figure 12. - Sample JA-27: Cross-sectional view looking SW showing asymmetric oxide grains in an oxide layer and S & C planes in a quartzite from Monte de Abajo Canyon. Gives top-to-NW shear sense. (5X; plain light)

Figure 13. - Sample JA-24: Cross-sectional view looking W showing a sigmoidal hornblende porphyroblast with a biotite tail on the top and stretched out hornblendes on its bottom in an amphibolite from Monte de Abajo Canyon. Gives top-to-N shear sense. (5X; plain light)

Figure 14. – Fold out map of study area with sketches of fabric relations in rocks and their sample locations from Monte Largo Canyon and Monte de Abajo Canyon.

a) Sample K99-ML-6: Cross-sectional view looking toward 040 showing 1) S_0/S_1 in hinge region of F_2 fold, 2) S_2 axial plane fabric parallel to MLSZ indicating shearing in MLSZ related to folding in upper plate, 3) garnets overgrowing S_1 & S_2, and 4) new shear along S_0/S_1 (reactivation) during S_3 and may have caused bending of S_2 around post S_2 garnets.

b) Sample J-16: Cross-sectional looking toward 040 showing 1) S_1 being crosscut and bending into S_2, 2) garnet overgrowing S_1 & S_2, and 3) F_3 folds folding S_1 & S_2 fabrics. Indicates top-to-NW shear sense on S_2.

c) Sample J-11: Cross-sectional view looking toward 050 showing 1) top-to-NW shear sense on S_2, 2) chloritoid growth as syn to post shearing, and 3) S_3 crenulations in S_2 fabric.

d) Sample J-18: Cross-sectional view looking toward 060 showing 1) top-to-NW shear sense on S_2, 2) garnets are syn to post S_1, 3)S_3 shear bands also giving top-to-NW shear sense, and 4) a possible earlier $S_{1(a)}$ fabric inside garnets.

e) Sample JA-33: Cross-sectional view looking toward 090 showing 1) S_2 subhorizontal in hinge region of F_2 fold, 2) quartz inclusions in garnets indicating garnets growth is post-S_2, and 3) S_3 and S_4 crenulations.

f) Sample JA-34: Cross-sectional view looking toward 040 showing 1) S_2 subhorizontal in hinge region of F_2 fold and crenulating S_1, 2) S_3 crenulation patterns in inclusions in chloritoid indicating later growth, and 3) S_4 crenulations as being much tighter than S_3 crenulations.

g) Sample JA-35: Cross-sectional view looking toward 040 showing 1) S_2 subhorizontal in hinge region of F_2 fold and offsetting S_1, 2) garnets as inclusions in chloritoid, and 3) broad S_3 crenulations and tight S_4 crenulations.

h) Sample JA-36 Plan view showing 1) garnet inclusion fabric ~35° from dominant S_2 fabric implying rotation of garnets, and 2) broad S_3 crenulations and tight S_4 crenulations.

i) Sample JA-37: Plan view showing 1) garnet, staurolite and chloritoid overgrowing S_3 crenulation fabric and 2) broad S_3 crenulations and tight S_4 crenulations.

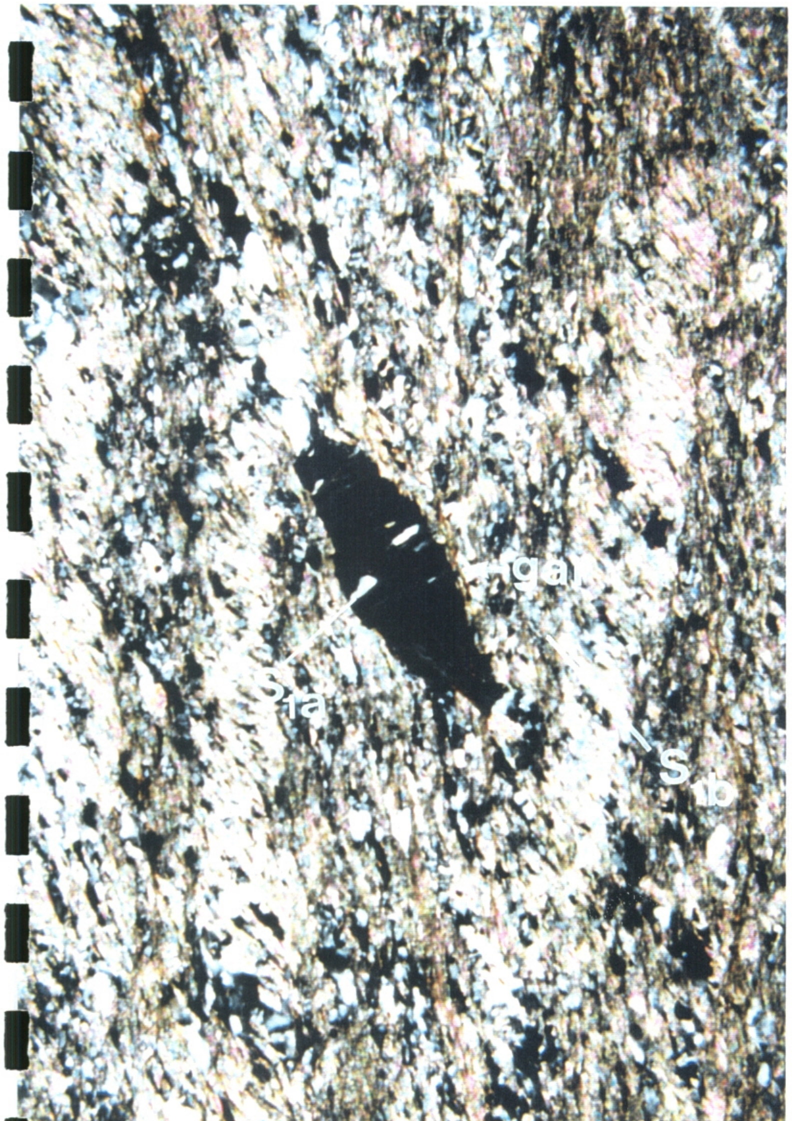

Figure 15. - Sample J-18: Cross-sectional view looking SW showing an elongate garnet in S_1 foliation with chlorite pressure shadow on upper end and perpendicular inclusions of quartz in a schist from S of MLSZ. Since inclusions must be younger they are labeled $S_{1(a)}$ and the elongation foliation as $S_{1(b)}$. (2.5X; cross polars)

Figure 16. - Sample J-16: Cross-sectional view looking SW showing F_3 folds in S_1 and S_2 foliation (mica band) in schistose quartzite S of MLSZ. Also note how S_1 layers are being bent into the S_2 foliation. (2.5X; plain light)

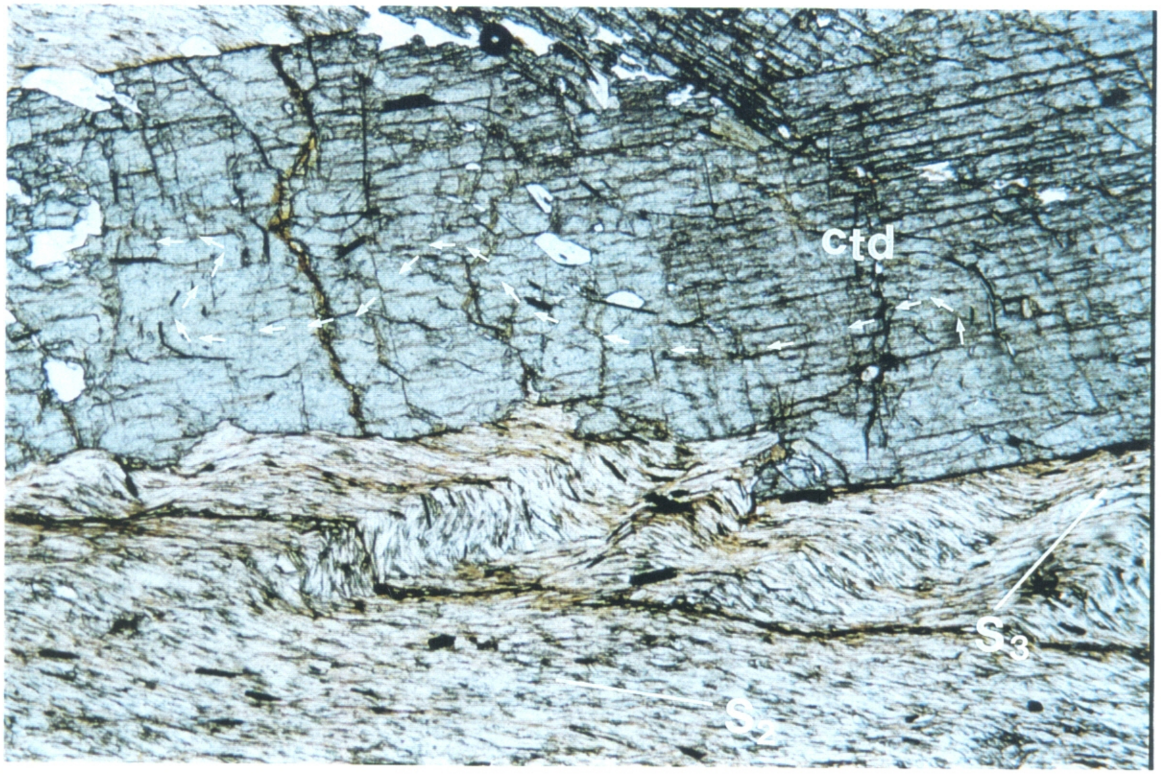

Figure 17. - Sample JA-34: Cross-sectional view looking NE showing oxide inclusions in chloritoid that are folded implying that S_3 crenulations were earlier than chloritoid growth in a garnet chloritoid schist from Monte de Abajo Canyon. Note how crenulations are much tighter outside of the chloritoid than inside. (5X; plain light)

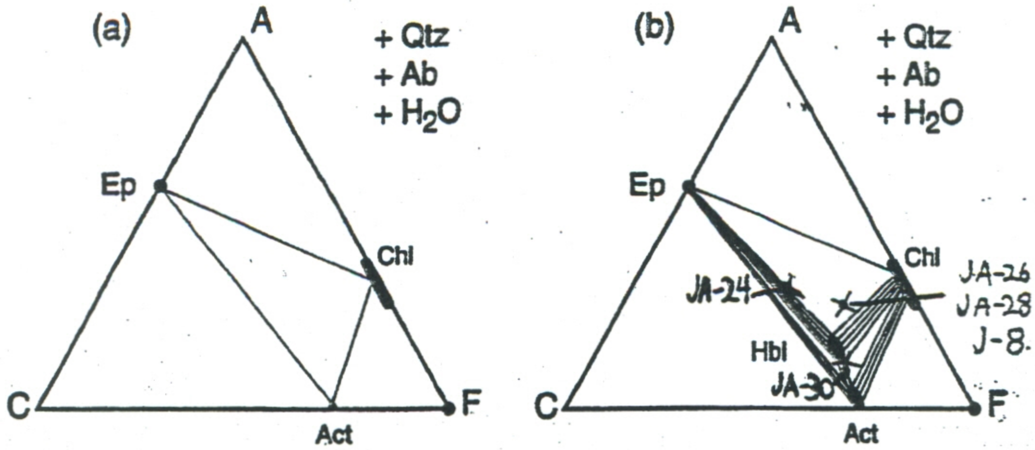

Figure 18. - ACF diagrams showing a) greenschist facies with the assemblage as chlorite + actinolite + epidote + plagioclase + quartz and b) amphibolite facies with the assemblage hornblende + epidote + chlorite + plagioclase + quartz, along with sample compositions of amphibolites from this study. Adapted from Spear (1993).

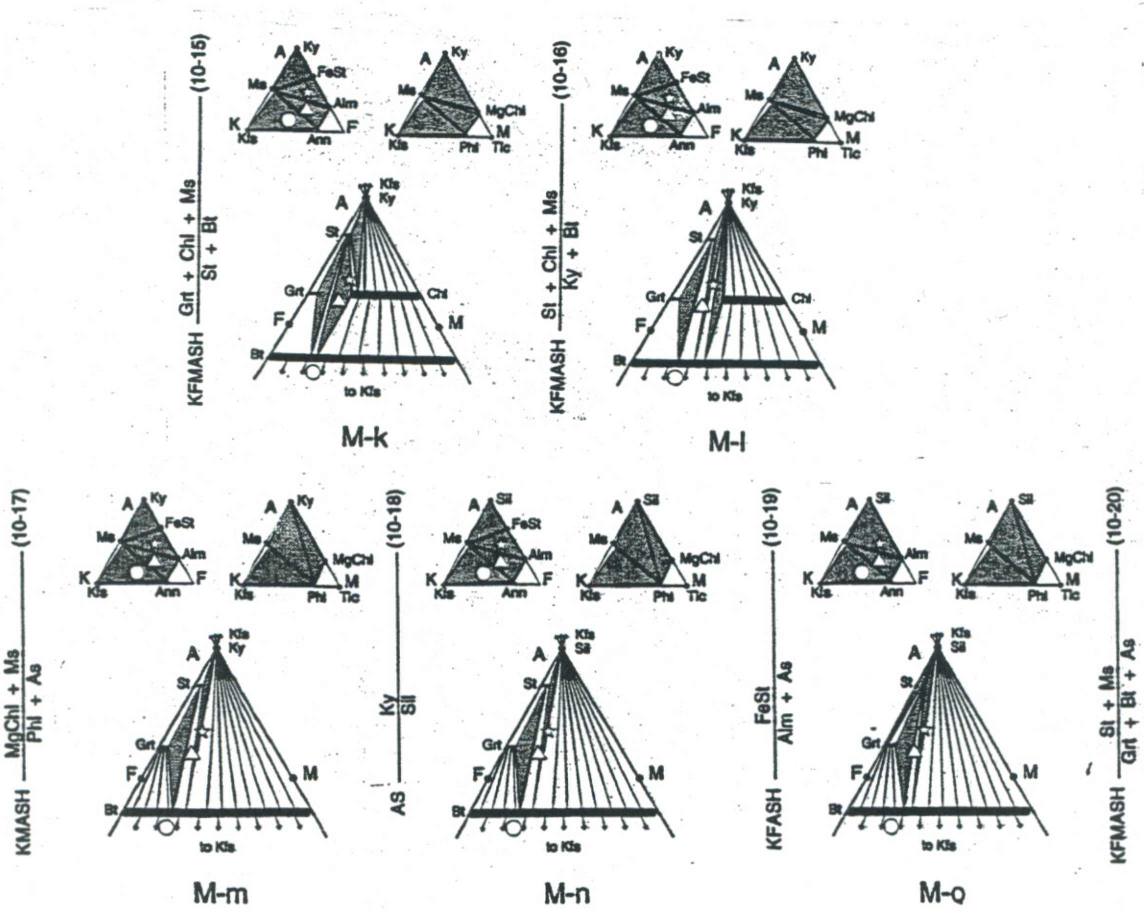

figure 19. - AKF, AKM & AFM diagrams showing the stability range for pelitic schists from Monte de Abajo Canyon. The star, triangle and circle represent hi-Al pelites, lo-Al pelites and granitic bulk compositions, respectively. Adapted from Spear (1993).

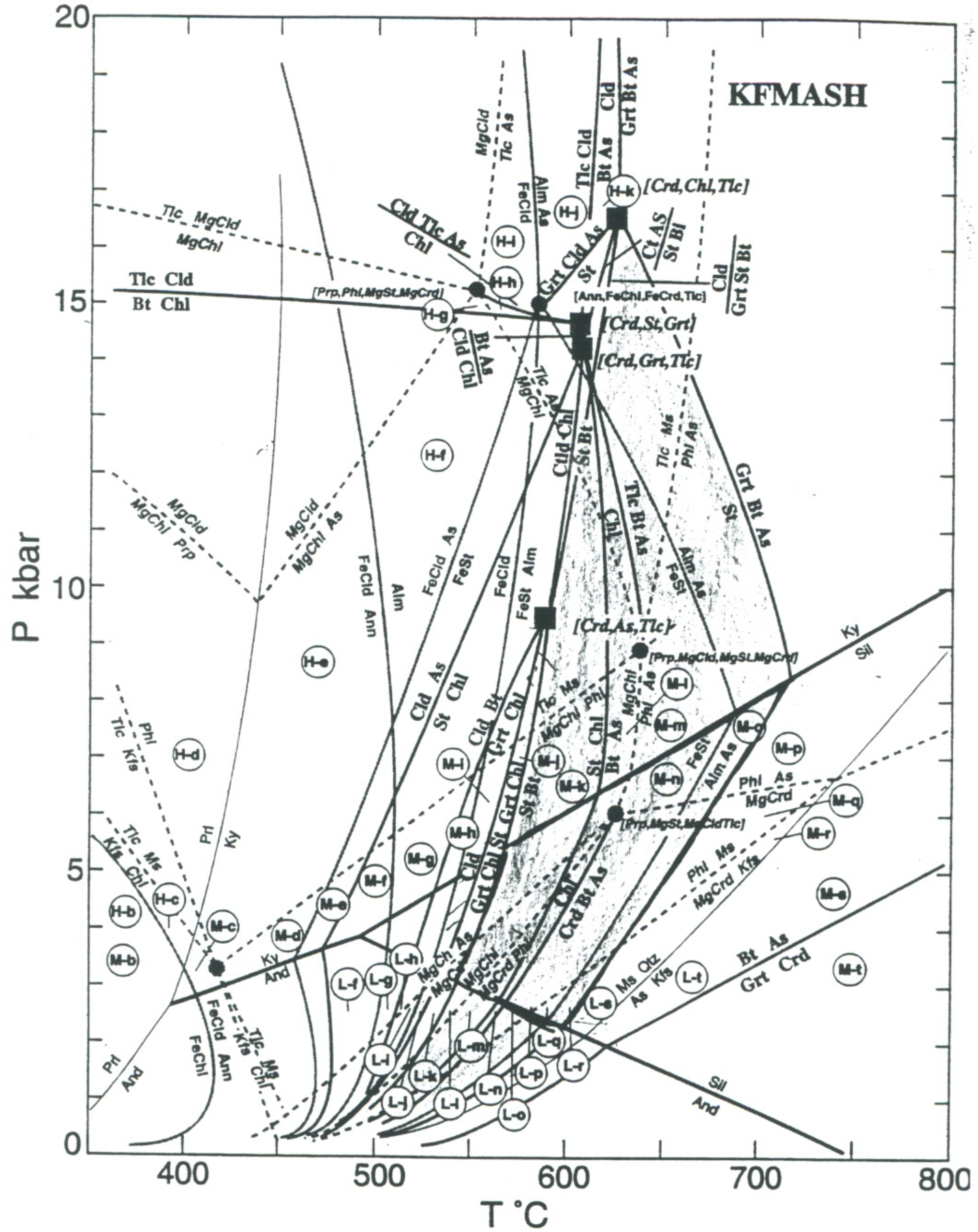

figure 20. - P-T grid for pelites in the KFMASH system. KFASH and KMASH reactions are in solid and dashed lines respectively. Shaded area is the probable stability range for pelitic schists from Monte de Abajo Canyon. From Spear (1993).

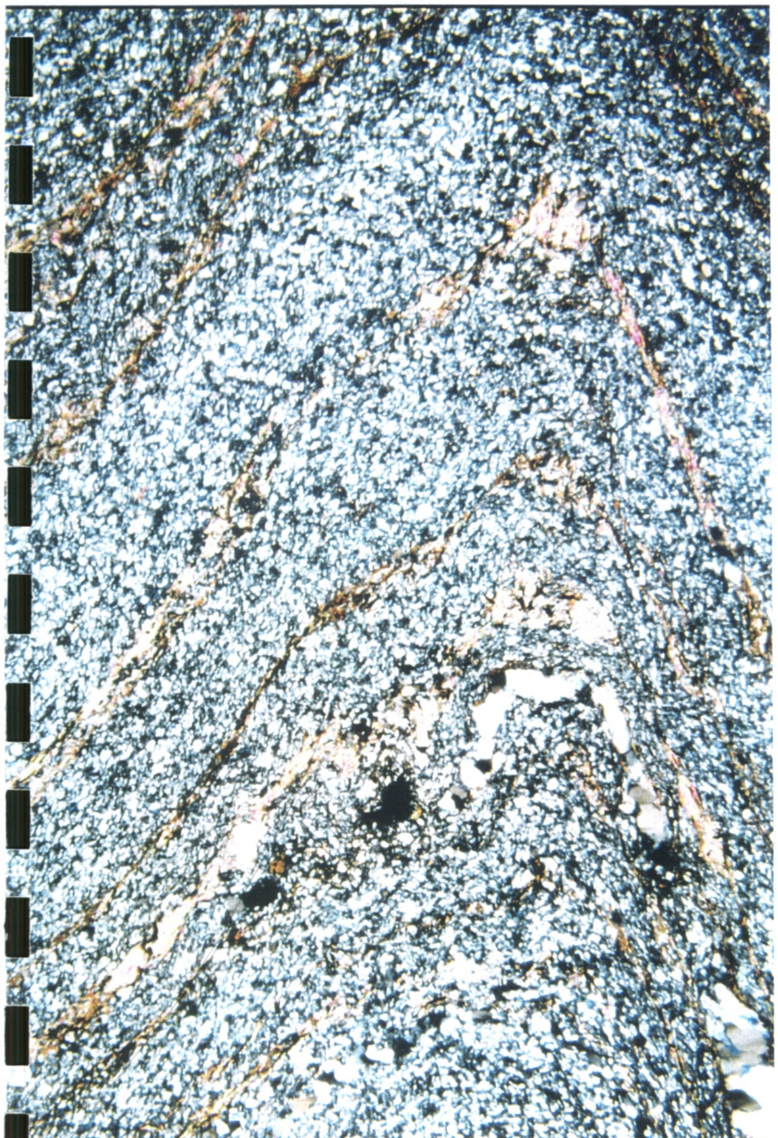

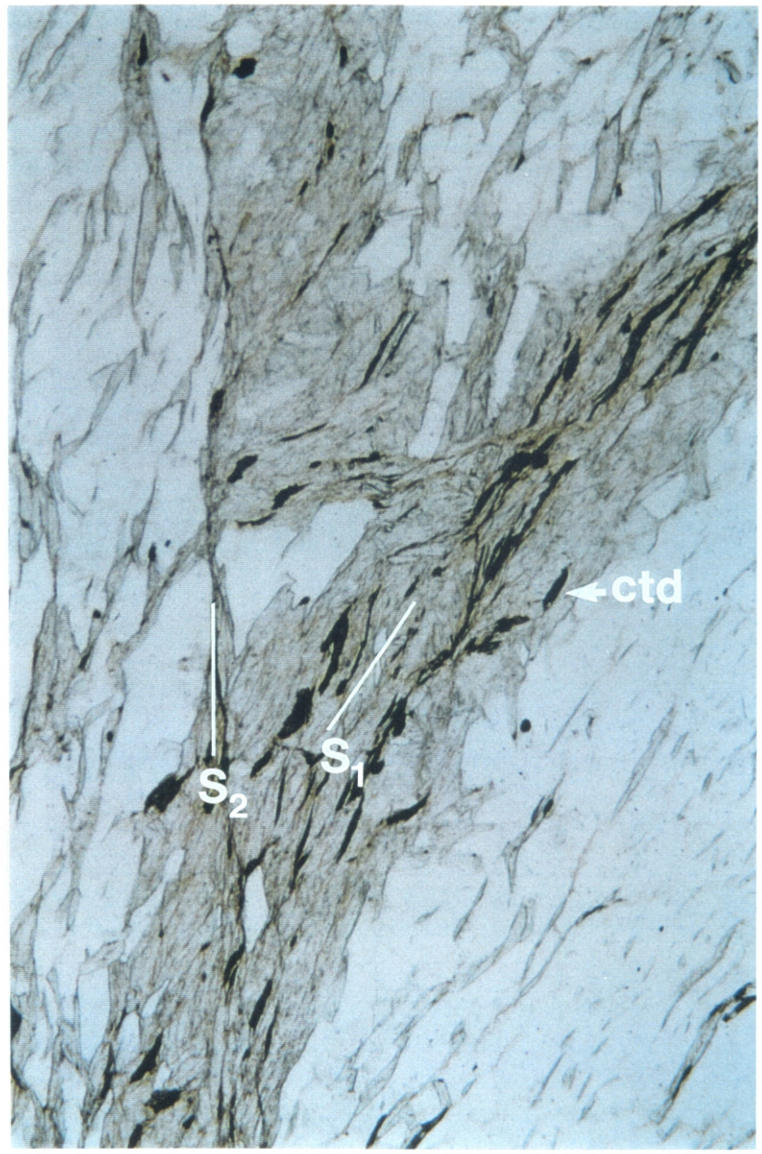

Figure 21. - Sample J-5: Cross-sectional view looking SW showing a folded mylonitic fabric. believed to be F_2 folds folding S_1 mylonitic fabric in quartzite from the MLSZ. (2.5X; cross polars)

Figure 22. - Sample J-11: Cross-sectional view looking NE showing chloritoid grains aligned in S_1 foliation in schistose quartzite S of MLSZ. These grains are interpreted to have grown under greenschist facies conditions. (5X; plain light)